



ARID Journals

ARID International Journal for Science and Technology (AIJST)

ISSN: 2662-009X

Journal home page: <http://arid.my/j/aijst>

ARID

International Journal for Science and Technology

مجلة أريد الدولية للعلوم والتكنولوجيا

VOL.7 NO.13 JUNE 2024

ISSN: 2662-009X

ARID
INTERNATIONAL
JOURNAL FOR SCIENCE AND
TECHNOLOGY

مجلة أريد الدولية للعلوم والتكنولوجيا

المجلد 7 ، العدد 13، حزيران 2024 م

Cytotoxic Effect of Biosynthesized Manganese Oxide Nanoparticles on Human Skin Squamous Carcinoma Cell Line (HSSCC) *in vitro*

Laith Ahmad Yaaqoob¹, Hind Hussein Obaid^{2*}, Zainab Farhan Ali³, Khawlah Jebur Khalaf³,
Raghad Akram Aziz⁴

¹Dep. of Biotechnology, College of Science, University of Baghdad, Baghdad , Iraq.

²Dep. of Biology, College of Science, University of Baghdad, Baghdad , Iraq.

³Dep. of Biology, College of Science, Al-Mustansiriyah University, Baghdad, Iraq.

⁴Dep. of Science, College of Basic Education, Al-Mustansiriyah University, Baghdad, Iraq.

التأثير السمي الخلوي لجسيمات المنغنيز النانوية المصنعة حيويًا في خط خلايا سرطان الجلد الحرشفي البشري خارج الجسم الحي

ليث أحمد يعقوب¹، هند حسين عبيد^{2*}، زينب فرحان علي³، خولة جبر خلف³، رغد أكرم عزيز⁴

¹قسم التقنيات الأحيائية، كلية العلوم، جامعة بغداد، بغداد، العراق.

²قسم علوم الحياة، كلية العلوم، جامعة بغداد، بغداد، العراق.

³قسم علوم الحياة، كلية العلوم، الجامعة المستنصرية، بغداد، العراق.

⁴قسم علوم الحياة، كلية التربية الأساسية، الجامعة المستنصرية، بغداد، العراق.

Hind_3000@yahoo.com

Arid.my/0003-5731

<https://doi.org/10.36772/arid.aijst.2024.7136>

ARTICLE INFO

Article history:

Received 03-06-2024

Received in revised form 10-06-2024

Accepted 11-06-2024

Available online 15-06-2024

<https://doi.org/10.36772/arid.ajst.2024.7136>

ABSTRACT

The current study intended to biosynthesis of manganese oxide nanoparticles (MnO -NPs) depending on prodigiosin pigment as stabilizing and reducing agent. which produced from environmental isolate of *Serratia marcescens* . The study of the biosynthesis of MnO NPs was characterized by different techniques, such as (UV-VIS, XRD, AFM, FE-SEM and FTIR). The results refer, the wavelength of biosynthesis of MnO NPs by using UV-VIS was (284 nm), the average volume was (45) nm). and image FE-SEM shows that the MnO- NPs mainly consists of nanosheets assembled in flower-like shape with different diameters.

The cytotoxic effects of (MnO -NPs) on Human Skin Squamous Carcinoma Cell Line (HSSCC) was significant ($p \leq 0.05$) comparative with control viability 100%. Maximum effective concentration were 4000 $\mu\text{g/ml}$ for 72hr exposure time which gave the highest inhibition rate 95% comparative with viability control 100%, but the minimum concentration was 3.9 $\mu\text{g/ml}$ which induced proliferation of (HSSCC)cells. So when the exposure time and the concentration was increased, the inhibition rate was increased.

Keywords: *Serratia marcescens*, Human skin squamous carcinoma cell line, cytotoxic effect, prodigiosin, MnO –NP.

المخلص

هدفت الدراسة الحالية إلى تخليق جسيمات أكسيد المنغنيز النانوية (MnO-NPs) حيويًا بالاعتماد على صبغة البرديوسين كعامل تثبيط ومختزل والتي أنتجت من العزلة البيئية *Serratia marcescens*. درست خصائص أكسيد المنغنيز المصنع حيويًا بتقنيات مختلفة مثل (UV-VIS, XRD, AFM, FE-SEM). تشير النتائج إلى أن الطول الموجي UV-VIS كان (284 نانومتر)، ومتوسط الحجم (45 نانومتر). وتظهر الصورة FE-SEM أن MnO-NPs يتكون بشكل أساسي من صفائح نانوية مجمعة في شكل يشبه الزهرة بأقطار مختلفة.

كانت التأثيرات السمية الخلوية لجسيمات المنغنيز النانوية في خط خلايا سرطان الجلد الحشفي البشري (HSSCC) معنوية ($p \leq 0.05$) مقارنة مع معاملة السيطرة التي أعطت نسبة حيوية 100%. كان التركيز الأفضل هو أعلى تركيز 4000 ميكروغرام/مل لمدة تعريض 72 ساعة مما أعطى أعلى معدل تثبيط نمو، فقط بلغ 95% مقارنة بحيوية السيطرة 100%. أما أقل تركيز مستخدم 3.9 ميكروغرام/مل فقد أدى إلى تكاثر خلايا (HSSCC). لذلك نستنتج أن زيادة زمن التعرض والتركيز، يزيد من معدل التثبيط.

الكلمات المفتاحية: بكتيريا سرشيا، خط خلايا سرطان الجلد البشري، التأثيرات السمية الخلوية، البرديوسين، جسيمات أكسيد المنغنيز النانوية.

1. Introduction

Cancer has emerged as the main cause of mortality worldwide. It is a deadly disease that kills millions of people each year, one in every two males and one in every three females is affecting, and kills one in every four women during their lives[1]. Despite the presence of various therapy options, cancer remains an issue for scientists. The research institutes and researchers moved to uncover alternative remedies for the existing medications and adopted a different method that may have a high chance of eradication the condition. Commercial pharmaceuticals are expensive to import, and their effectiveness deteriorates over time due to cancer cell resistance to these medications [2]. Therefore, many countries worldwide focused much attention to the biosynthesis nanoparticles as the natural source of drugs [3]. The discovery of biosynthesized nanoparticles' anticancer effect gave it enormous medical relevance, because biosynthesized nanoparticles are biotherapeutic agents for several types of human tumors. Nanotechnology and nano-biomedicine are the ability to compute, display, manipulate, and generate goods on an atomic size, typically ranging from 1 – 100 nanometers. [4]. Nowadays, electrical device efficiency and reduction are quite essential as compared to other factors, and nanomaterials play a significant part in this. Everyone is interested in nanotechnology because of its numerous applications ranging from fabric to medicine, including its anticancer activity [5]. The most crucial aspect of this is the widespread use of nanoparticles in electronics, optics, microbiology, biotechnology, medicine, environmental remediation, and material sciences. The utilization of ecologically friendly raw materials, such as bacterial extracts, for the production of manganese oxide nanoparticles offers various environmental and economical benefits [6]. For pharmaceutical businesses and therapeutic aims, so they could avoid the employment of harmful chemicals in the manufacturing process [7]. The components found in the isolated bacteria are responsible for manganese reduction. Adequate

substrates can also be employed to decrease bacterium extracts, such as manganese sulfate. Biological nanotechnology is quite interesting and involves a wide range of techniques that limit or eliminate dangerous pollutants to environmental preservation. [8]. Biological manufacturing has more benefits than physical and chemical approaches so it is easier to process, less expensive, and more scalable for the large-scale manufacturing [9]. Manganese oxide nanoparticles are the first choice for biological and medical specialized applications because to their biocompatibility, superparamagnetic properties, and chemical stability [10]. The aim of study was to investigate the cytotoxic effects of biosynthesized manganese oxide-nanoparticles on HSSCC cell line.

2. Experimental Procedure

2.1 Production of Prodigiosin pigment

Fermentation medium preparation is often based on [15]. This media contain on peptone (5 g/L) used as nitrogen source, sucrose (10 g/L) used as carbon source, $\text{MgSO}_4 \cdot 7\text{H}_2\text{O}$ (0.61 g/L), $\text{MnSO}_4 \cdot 4\text{H}_2\text{O}$ (2 g/L), $\text{CaCl}_2 \cdot 2\text{H}_2\text{O}$ (8.82 g/L), and $\text{FeSO}_4 \cdot 4\text{H}_2\text{O}$ (0.33 g/L) were used to make the medium. Before autoclaving the pH was adjusted to 7.0. Following sterilization, the medium was allowed to cool before inoculating 2% of *Serratia marcescens* isolate, 0.5 McFarland (1.5×10^5 CFU/ml) and cultivated in a shaker incubator at 120 Revolutions /minute (rpm), at 28 °C for 48 hrs. [11] [12].

2.2 Extraction of Prodigiosin Pigment

After 48 hour of culture incubation, the crude prodigiosin was extracted by centrifuge at 8000 rpm for 15 minutes. After discarding the supernatant, methanol 250 ml was added to the collecting cells and mixed carefully for 3 hr at room temperature. The resultant mixture then centrifuged at 8000 rpm for 20 minutes, the supernatant collected and filtered with 0.2 m Whitman filter paper. The methanol filtrate was concentrated at 70 °C by using a rotary evaporator, and the red pigment

was extracted using double amount of chloroform. In a reparatory funnel, the two solvents were violently combined; the chloroform phase which is (organic phase) was recovered and then the supernatant was kept in a dark bottle in the refrigerator [13].

2.3 Biosynthesis of manganese oxide nanoparticles

Manganese oxide nanoparticles were created employing the biosynthesis method and manganese sulfate $MnSO_4$ (Indian) in the creation of manganese oxide nanoparticles. It was made by adding 5 gm manganese sulfate $MnSO_4$ to (50 ml) crud prodigiosin solution then dispersing it in an ultrasonication bath for 60 minutes, the pH was adjusted to 7.0 and then left overnight in the darkroom. The solution comprises manganese oxide-NPs were concentrated and separated by centrifugation for 30 minutes at 6000 rpm after being rinsed twice with deionized distilled water (DDW) then precipitated by centrifugation for 30 minutes at 6000 rpm. The powder was dried at $40^{\circ}C$ in an oven for 24 hr and stored in a dark container.

2.4 Characterization of biosynthesized MnO –nanoparticles

- Fourier-transform infrared spectroscopy (FTIR)
- UV-Vis spectra analysis.
- Scanning electron microscope (SEM).
- Atomic force microscopy (AFM) analysis.
- X-RAY Diffraction method analysis (XRD).

2.5 The Cytotoxic effects of biosynthesized manganese oxidenanoparticles on HSSCC cell line

2.5.1 Type of the studied Cancer Cell Line

This study was used the Human Skin Squamous Carcinoma (HSSCC) cell line, passage number 27 cell lines were used.

The cells raised on tissue culture media that contained RPMI-164, which was provided by the Sigma (USA) firm along with 5% Fetal Calf Serum (FCS) which was also provided by the Sigma company (USA).

2.5.2 Cytotoxicity assay

This experiment was conducted using multiple (96) flat-bottomed tissue culture microtiter plates by these stages:

1-Cell seeding:

-After the cells had grown and multiplied, the monolayer-containing containers were removed, and the cells then harvested by using a solution of 2ml Trypsin-Versin (T.V).

- Each container received 20 ml of the culture medium containing the serum, which was added and thoroughly mixed. Following that, the cells were counted using aHaemocytometer and1% Trypan blue dye as suggested by Freshney [13].

- suspension of(0.1) ml cells were pipetted into each well of the plate using a micropipette 1×10^4 cells/well were present in each well. The surface of the plate was then coated with a specially created piece of transparent, sterile adhesive paper, and the plate was gently shifted before being incubated at 37°C overnight to facilitate cell adhesion.

2- Exposure of cell line to the MnO-NPs

The following day after seeding, the serial dilutions of Mn-O NPs were carried out in sterilized test tubes using RPMI-1640 Serum free medium. The dilutions were started gradually and ranged from 1/2 to 1/2048, yielding concentrations ranging from 4000 to 3.9 µg/ml, respectively. Once the adhesive paper was removed, poured the culture media from the wells.

Since 0.2 ml serum-free culture medium was then added to column No. 1, it was used as a negative control. In contrast, MnO-NPs dilutions that prepared as (0.2 ml/well/concentration) were added to columns from 2 to 12 the dilutions of Mn-NPs, and a fresh layer of adhesive paper was then poured on the surface of plate. The plates then exposed for 24, 48, and 72 hours each hour at a temperature of 37°C.

3- Cytotoxicity

Using MTT stain to investigate the cytotoxic effect of MnO-NPs on cells as following:

All plates were removed after each incubation time, their contents were drained out, and they were then rinsed with Phosphate Buffer Saline (PBS) solution. Each well then received 0.1 ml of MTT stain, which was applied and allowed to sit for 20 minutes. The excess dye was subsequently removed from the cells by repeat PBS solution washings. The ELISA microplate spectrophotometer was used to read the data once the plates had fully dried. It operates at 492 nanometers wavelength. The Inhibitory Rate (I.R) was calculated [15], and the Proliferation Rate (P.R.) was measured [16] as below:

$$\text{IR}\% = \frac{A - B}{A} \times 100 \dots\dots\dots (1)$$

$$\text{PR}\% = \frac{B}{A} \times 100 \dots\dots\dots (2)$$

IR= Inhibitory Rate

PR=Proliferation Rate

A= Absorbency for Negative Control

B= Absorbency for Test

2.6 Statistical analysis

The Statistical Analysis System-SAS (2018) program was used to detect the effect of difference factors in study parameters. Least significant difference (LSD) test analysis of variation (ANOVA) was used to significant compare between means in this study. A value of $P \leq 0.05$ was considered statistically significant.

3. Results and Discussions

3-1 Production of Prodigiosin Pigment

After 48hr in the shaker incubator, the manufacture of prodigiosin began. The prodigiosin concentration was around 0.71 g/L after four runs, at the conclusion of the stationary phase (after 48 hr. incubation) and after 45 hr during the stationary phase it reached a high of 0.83 g/L. During The medium gradually became red during the incubation, due to the accumulation of prodigiosin, that occurred mostly in the stationary phase.

3-2 Characterization of biosynthesized MnO –nanoparticles

FTIR Spectrum for MnO- NPs

Figure (1) shows the FTIR spectra of MnO NPs. Broad absorption is frequent in the wavelength ranges between 4000 and 3000 cm^{-1} are allocated both the stretching collision of H–O–H and hydroxyl absorption, while the peak detected at 1631 cm^{-1} symbolized the bending collision of adsorbed water. The peaks 420.45-649.97 cm^{-1} referred to the Mn–O vibrations of MnO₆

octahedra in α -MnO₂. Additionally, the wavelength of the absorption peak near 1139.85 cm⁻¹ and 823 cm⁻¹ conferred the surface -OH groups of Mn-OH for colloidal MnO -NPs.

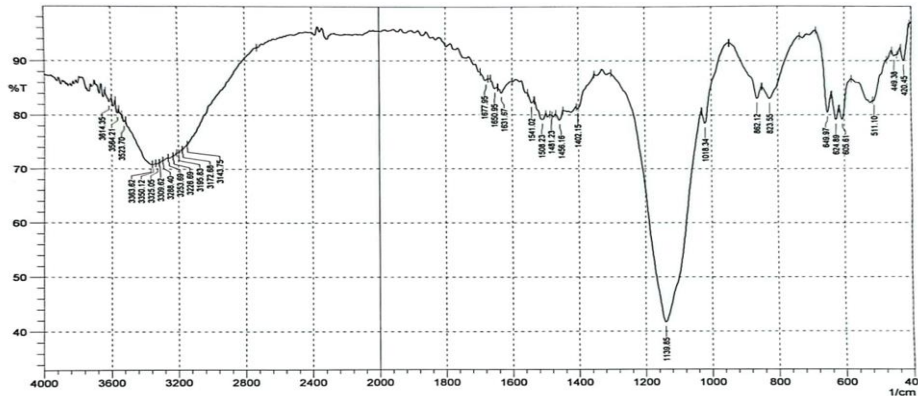


Figure (1):FTIR Spectrum for MnO-NPs.

UV-vis spectra of MnO-NPs

Figure (2) reveals the absorbance bands of MnO at a wavelength around 300-900 nm. The results observed that the absorbance spectra of biosynthesis MnO using extracts has sharply absorbance with the highest peak at 348 nm.

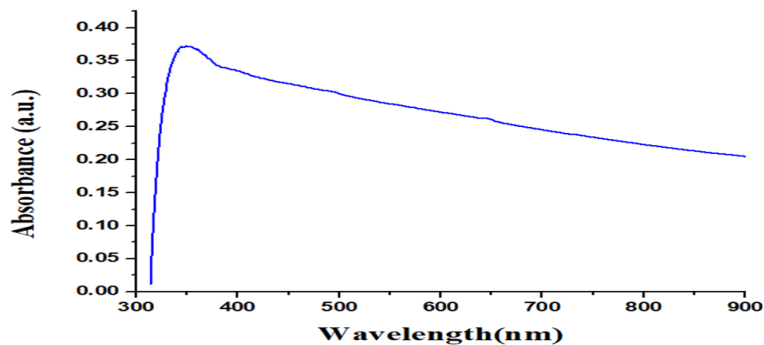
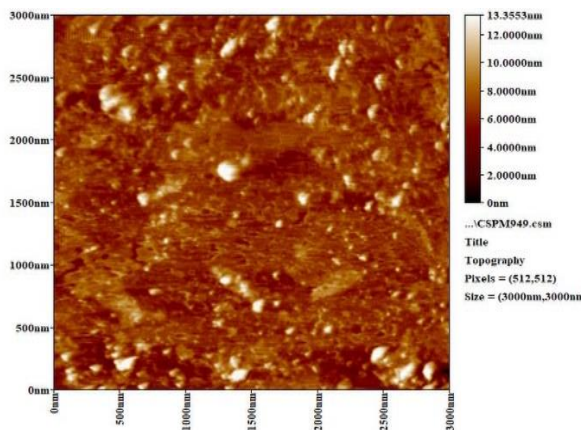


Figure (2):UV-vis spectra of MnO-NPs.

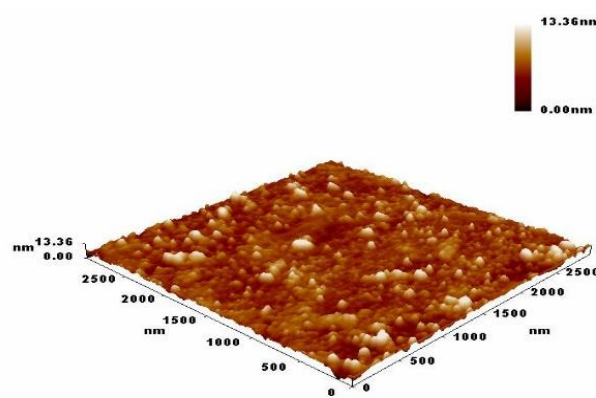
Atomic force microscopy (AFM)

Atomic force microscopy (AFM), the surface shape of the biosynthesized MnO NPs was estimated by atomic force microscopy to explain that MnO-NPs 2D and 3D [24]. AFM images show that the synthesized MnO-NPs are flower-like shape. The size of an average diameter of 45.01 nm was also measured by AFM (Fig 3).

| | |
|---|--|
| Sample: MnO Line No.: line 1 Instrument: CSPM | Code: Sample Code Grain No.:3424 Date:2022-11-12 |
| Avg. Diameter: 45.01 nm <=50% Diameter:40.00 nm | <=10% Diameter:26.00 nm <=90% Diameter:68.00 nm |



3D



2D

Figure (3): Average size of MnO NPs biosynthesized by using Prodigiosin illustrate 2D and 3D topological by AFM.

FE-SEM of Biosynthesized MnO-NPs

Figure (4) shows the FE-SEM analysis images of high-density MnO prepared using a biosynthesis method. It shows that the product mainly consists of nanosheets assembled in flower-like shape with different diameters.

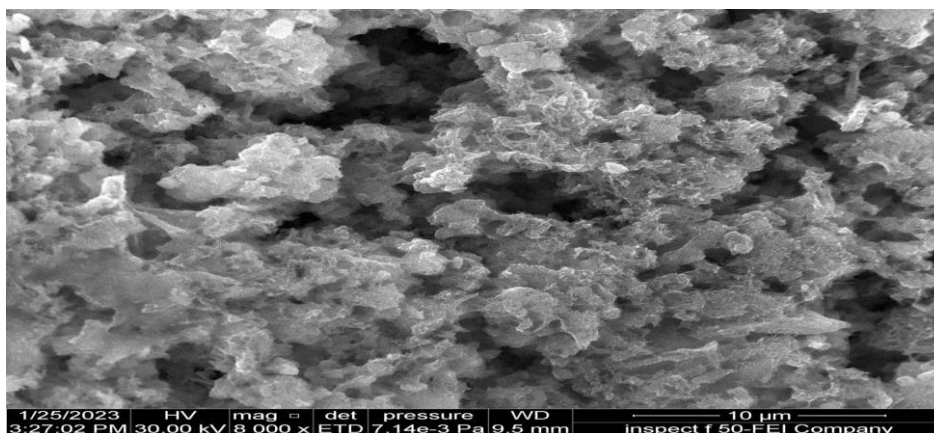


Figure (4): FE-SEM Images of MnO- NPs.

XRD of Biosynthesized MnO NPs

Figure (5) explains the XRD patterns of α - \square -, \square -, and \square -, \square - MnO-NPs. The diffraction peaks in the XRD patterns corresponded to the 110, 200, 310, and 211 Miller indices of α -MnO (JCPDS No. 44-0141), in the XRD patterns the diffraction peak correspond to (002) crystal plane of \square -MnO (JCPDS No. 18-0802), the diffraction peak in the XRD patterns correspond to the 120 crystal plane of \square -MnO –NPs (JCPDS No. 44-142), the diffraction peak in the XRD patterns correspond to the 110 crystal plane of \square - MnO –NPs (JCPDS No. 24-0735). The average crystallite size (D) of MnO NPs is 45 nm.

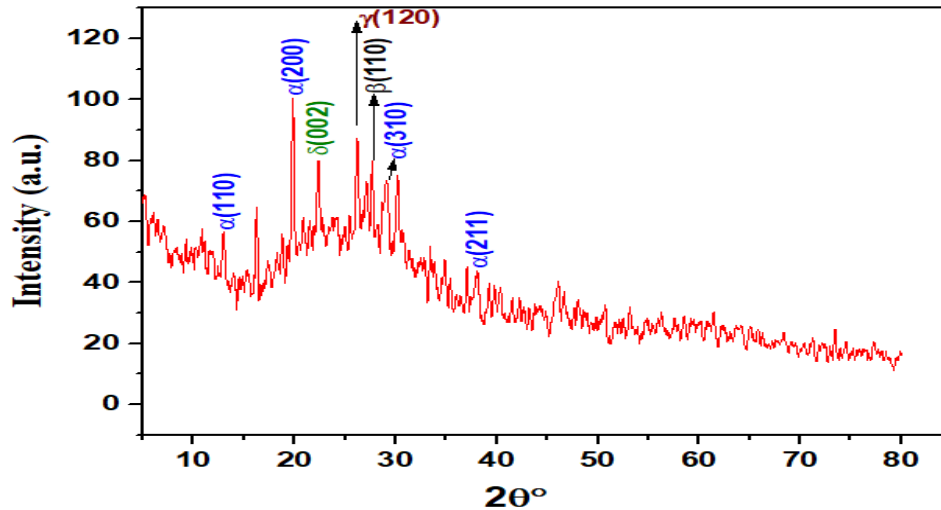


Figure (5): XRD of MnO- NPs.

3-3 Cytotoxic effect of biosynthesized MnO NPs on HSSCC cell line

In this study eleven concentrations of MnO -NPs were used at three time of exposure (24,48 and 72) hr on HSSCC cell line (Fig. 9). The result was significant ($p \leq 0.05$). The best concentration was 4000 $\mu\text{g/ml}$ after 72 h (Fig. 8) which was the best exposure time and the inhibition rate was 95% comparative with the control 100% viability, when the exposure time was decreased the inhibition rate was decreased also and was 89% and 77% after 48 ,24 hr respectively(Fig. 6 and 7). The concentration 250 $\mu\text{g/ml}$ was the minimum concentration that inhibit the growth of cancer cells after (24, 48 and 72) hr with inhibition rate (28,37 and 58)% respectively comparative with the control 100% viability. But when the exposure time was increased and the concentration was decreased this was induced cell proliferation so minimum concentration of MnO -NPs (3.9 $\mu\text{g/ml}$) at 72hr gave the high cell proliferation 110%.

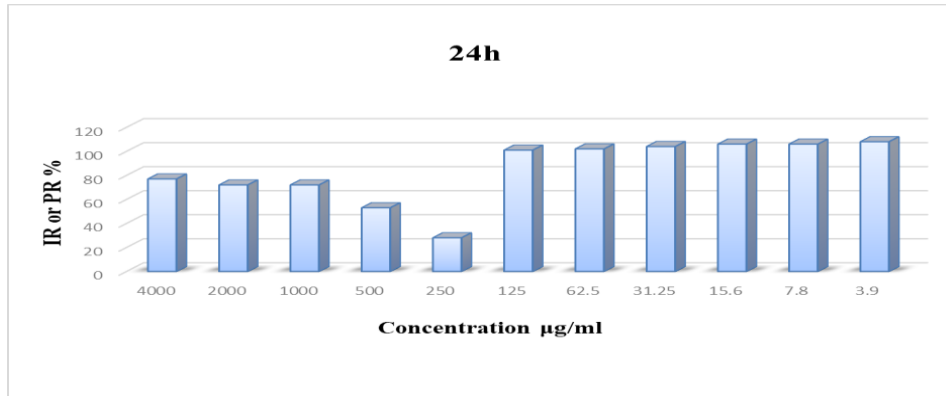


Figure (6): Cytotoxic effect of MnO-NPs on HSSCC cell line after 24 hr exposure time.

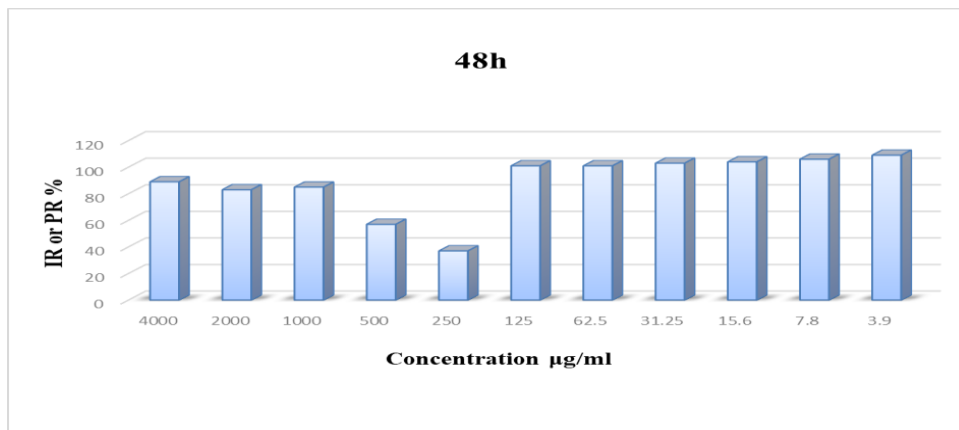


Figure (7): Cytotoxic effect of MnO-NPs on HSSCC cell line after 48 hr exposure time.

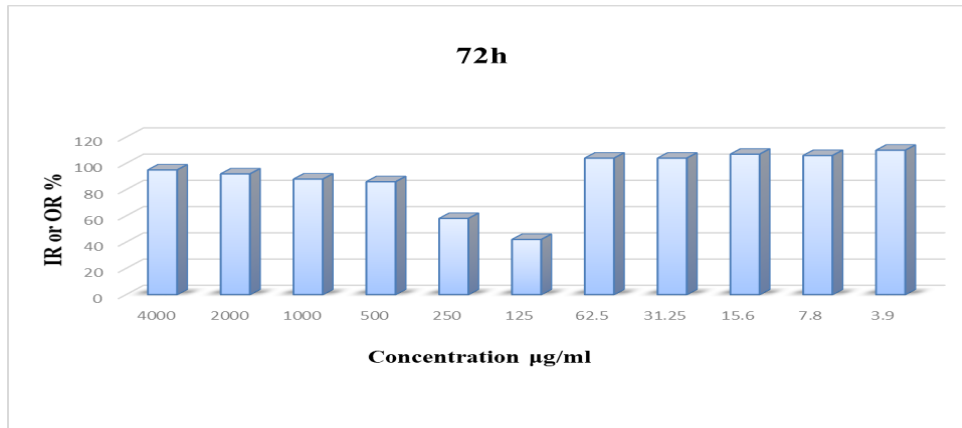


Figure (8): Cytotoxic effect of MnO-NPs on HSSCC cell line after 72 hr exposure time.

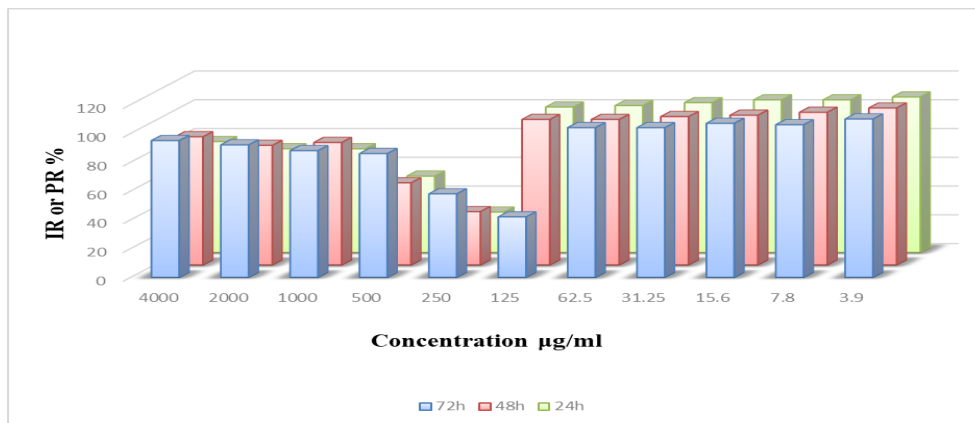


Figure (9): Comparative cytotoxic effect of MnO-NPs on HSSCC cell line after (24, 48, 72) hr exposure time.

In this study eleven concentrations of MnO -NPs were used at three time of exposure (24,48, and 72)hrs on Human skin squamous carcinoma cell line . The result was significant ($p \leq 0.05$). The best concentration was 4000 µg/ml after 72 h exposure time. A previous study using MnO -NPs by Bonet-Aleta [17] showed significant cytotoxic result on cancer cell because Manganese oxide nanoparticles offer unique advantages in terms of redox properties and specificity: low O₂ concentrations, mildly acidic pH and high oxidative stress; environmental conditions that often lead to a reduction in the efficacy of cancer treatments [18]. Ding *et al.* and Nie, et al. explained

that the use of inorganic nanomaterials to tackle and exploit the intrinsic chemical nature of the cancer cell and has emerged as a promising strategy in cancer therapy due to the rich surface chemistry of MnO NPs enabled the proper interaction with cell wall and increase its permeability and also damage key molecules in cell, such as DNA or proteins, entailing cell apoptosis and death [19] [20]. Ghosh revealed that the activity of inorganic Mn-based nanocatalysts in heterogeneous catalysis depends on multiple physicochemical factors: size, shape, surface properties (like charge, composition or ligands), crystalline order or stability (pH, temperature) [21]. MnO NPs possess good biocompatibility and low toxicity at certain levels so it can use in nanomedicine [22] [23].

4. Conclusion

The cytotoxic effect of MnO -NPs on HSSCC cell line was effective after 72 hrs exposure time. when the concentration and the exposure time when increased; the inhibition rate was increased also, but when the concentration was decreased this was induced cell proliferation.

List of Abbreviations:

DDW → Deionized Distilled Water.
 AFM → Atomic force microscopy.
 FTIR → Fourier-transform infrared spectroscopy
 HSSCC → Human Skin Squamous Carcinoma Cell Line.
 MnO NPs → manganese oxide nanoparticles.
 rp m → Revolutions /minute
 SEM → Scanning electron microscope.
 XRD..... → X-RAY Diffraction method analysis.

References

- [1] D.Nie, Zhu, Y.T. Guo, M.Yue, M. Lin, “Research advance in manganese nanoparticles in cancer diagnosis and therapy”, *Front. Mater*, 9 (2022) 73-85.
- [2] W.Bao, F.Tian, C.Lyu, B.Liu, B. Li, L.Zhang, X.Liu, F.Li, D.Li, X.Gao, “Experimental and theoretical explorations of nanocarriers multistep delivery performance for rational design and anticancer prediction”, *Sci. Adv*.7 (2021) 2458.
- [3] G.Y.Liou, P.Storz, “Reactive oxygen species in cancer”, *Free Radic. Res*, 26(2010) 479–496.
- [4] A.A. Yetisgin, S.Cetinel, M.Zuvin, A.Kosar, O. Kutlu, “Therapeutic nanoparticles and their targeted delivery applications” *Molecules*, 25 (2020) 2193.
- [5] T.Ganbold, S. Han, A. Hasi, H.Baigude, “Receptor-mediated delivery of therapeutic RNA by peptide functionalized curdlan nanoparticles”, *Int. J. Biol. Macromol*, 126 (2019) 633–640.
- [6] X. Jia, M.Guo, Q. Han, Y.Tian, Y.Yuan, Z.Wang, Y.Qian, W. Wang, “Synergetic tumor probes for facilitating therapeutic delivery by combined-functionalized peptide ligands”, *ACS Appl. Mater. Interfaces* , 92 (2020)5650–5655.
- [7] B.Guan, X.Zhang, “Aptamers as versatile ligands for biomedical and pharmaceutical applications”, *Int. J. Nanomed*, 15 (2020)1059–1071.
- [8] J.Hamilton, V.L.Marlow, R.A.Owen , M.D.A. Alcoforado –Costa, M.Guo, , and B.G. Etal, “A Holin and an Endopeptidase are Essential for Chitinolytic Protein Secretion in *Serratia marcescens*”, *Cell Biology* , 207, No.5(2014) 615-626.
- [9] Z. Zhang, Y.Ji, “Nanostructured manganese dioxide for anticancer applications: preparation, diagnosis, and therapy”, *Nanoscale*. 12 (2020) 17982–18003.
- [10] J. Bonet-Aleta, M. Sancho-Albero, J. Calzada-Funes, S. Irusta, P. Martin-Duque, J. L. Hueso, J. Santamaria, “Glutathione-triggered catalytic response of copper-iron mixed oxide nanoparticles. Leveraging tumor microenvironment conditions for chemodynamic therapy”, *J. Colloid Interface Sci*, 617 (2022) 704–717.
- [11] RM., kamel, and L.A.Yaaqoob, “Evaluation of the Biological effect synthesized Iron Oxide Nanoparticles on *Enterococcus faecalis*.” *Iraqi Journal of Agricultural Sciences*, 53 (2) (2022) 440- 452.
- [12] B. A.Forbes, D. F. Sahm, and A. S. Weissfeld, “Bailey and Scotts' Diagnostic microbiology St Louis”, Mosby (2007)¹²th. ed.
- [13] W. C.Chen, , W. J. Yu, C. C. Chang, J. S. Chang, S. H. Huang, C. H. Chang, and Y. H. Wei, “Enhancing production of prodigiosin from *Serratia marcescens* C3 by statistical experimental design and porous carrier addition strategy”, *Biochemical Engineering Journal*, 78 (2013)93-100.
- [14] R. I.Freshney, Culture of animal cells: “A manual for basic technique”, 4th ed. Wiley-Liss, A John Wiley and Sons, Inc. Publication, New York (2000).
- [15] S. Gao, B. Yu, Y. Li, W. Dong, H. Luo, “Antiproliferative effect of Octreotide on gastric cells mediated by Inhibition of Akt/PKB and telomerase”, *World J. Gastroentero*, 19 (2003) 2362-5.
- [16] J. Chumchalova, J. Smarda, “Human Tumor Cells are Selectively Inhibited by Colicins”, *Folia Microbiol*, 48 (2003)111-5.
- [17] J. Bonet-Aleta,.; J. Calzada-Funes,.; M.J.L. Hueso, “Manganese oxide nano-platforms in cancer therapy: Recent advances on the development of synergistic strategies targeting the tumor microenvironment” , *Elsevier journal*, 29 (2022) 101628.

- [18] Y.Guo,; Y.Xu,; Q.Bao,; C.Shen, D.Ni,; P.Hu,; J. Shi, “Endogenous copper for nanocatalytic oxidative damage and self-protection pathway breakage of cancer”, *ACS Nano*,15 (2021)16286–16297.
- [19] B.Ding,; P.Zheng,; P.A. J.Ma, Lin, “Manganese oxide nanomaterials: synthesis, properties, and theranostic applications”, *Adv. Mater*, 23 (2020)1905823.
- [20] D.Nie,;Y. Zhu,; T.Guo,; M.Yue,; M.Lin, “Research advance in manganese nanoparticles in cancer diagnosis and therapy”, *Front. Mater*,29 (2022)857385.
- [21] S.K.Ghosh, “Diversity in the family of manganese oxides at the nanoscale: from fundamentals to applications”, *ACS Omega*, 5 (2020)25493–25504.
- [22]A. H.Reaz,;S. Saha, C.K.Roy, M. A Wahab, G.Will;M. A. Amin,Y. Yamauchi,S. Liu, Y. V.Kaneti,., M.Hossain; S. H. Firoz, “Boosting capacitive performance of manganese oxide nanorods by decorating with three-dimensional crushed graphene”, *Nano Convergence*,9(2022)10.
- [23] Y.Ding,Y. Dai,M. Wu, L. Li, “Glutathione-mediated nanomedicines for cancer diagnosis and therapy”, *Chem. Eng. J.* 426 (2021)128880.